Wear-resistant and adherent nanodiamond composite thin film for durable and sustainable silicon carbide mechanical seals.

EGIZA, M., DIAB, M.R., ZIA, A.W., MURASAWA, K., FAISAL, N. and YOSHITAKE, T.

2024

Wear-resistant and Adherent Nanodiamond Composite Thin Film for Durable and Sustainable Silicon Carbide Mechanical Seals

Mohamed Egiza, Mohamed Ragab Diab, Abdul Wasy Zia, Koki Murasawa, Nadimul Faisal, Tsuyoshi Yoshitake

PII: S0043-1648(24)00159-5

DOI: https://doi.org/10.1016/j.wear.2024.205394

Reference: WEA 205394

To appear in: *Wear*

Received Date: 13 February 2024

Revised Date: 20 April 2024

Accepted Date: 1 May 2024

Wear-resistant and Adherent Nanodiamond Composite Thin Film for Durable and Sustainable Silicon Carbide Mechanical Seals

Mohamed Egiza [a, b,*], Mohamed Ragab Diab [a,c], Abdul Wasy Zia [d], Koki Murasawa [c,e], Nadimul Faisal [b], Tsuyoshi Yoshitake [c, **]

[a] *Department of Mechanical Engineering, Kafrelsheikh University, Kafrelsheikh 33516, Egypt*
[b] *School of Engineering, Robert Gordon University, Garthdee Road, Aberdeen AB10 7GJ, UK*
[c] *Department of Advanced Energy Science and Engineering, Faculty of Engineering Sciences, Kyushu University, Kasuga, Fukuoka 816-8580, Japan*
[d] *Institute of Mechanical Process and Energy Engineering (IMPEE), School of Engineering and Physical Sciences, Heriot-Watt University, Edinburgh EH14 4AS, UK*
[e] *OSG Corporation, 3-22 Honnogahara, Toyokawa, Aichi 442-8543, Japan*

Corresponding authors: Mohamed_Egiza@eng.kfs.edu.eg and Tsuyoshi_yoshitake@kyudai.jp

Abstract:

In response to environmental concerns, there is a growing demand for durable and sustainable mechanical seals, particularly in high-risk industries like chemical, petroleum, and nuclear sectors. This work proposes augmenting the durability and sustainability of silicon carbide (SiC) ceramic seals with the application of a nanodiamond composite (NDC) film through coaxial arc plasma deposition (CAPD) in a vacuum atmosphere. The NDC coating, with a smooth surface roughness of Ra = 60 nm as substrate, demonstrated a thickness of 1.1 μm at a deposition rate of 2.6 μm/hr. NDC film has demonstrated exceptional mechanical and tribological characteristics, such as a hardness of 48.5 GPa, Young's modulus of 496.7 GPa, plasticity index (H/E) of 0.098, and fracture toughness of H^3/E^2 = 0.46 GPa, respectively. These NDC films showcased commendable adhesion strength (> 60 N), negligible wear, and low friction (≤ 0.18) during dry sliding against a SiC counter material. Raman analysis has confirmed the nanocomposite structure of NDC film, emphasizing the role of highly energetic carbon ions in enhancing film adhesion by forming SiC intermetallic compounds at the interface through the diffusion of silicon atoms from the substrate into the films. The abundance of grain boundaries and rehybridization of carbon sp^3 to sp^2 bonding is perceived to improve tribological performance. CAPD excels in synthesizing long-life eco-friendly NDC coatings for durable and sustainable mechanical seals, featuring smooth surfaces, superior adhesion, outstanding hardness, and wear resistance, making them high potential candidates for various tribological applications.

Keywords: Dry friction; Wear-resistance; Mechanical seals; Nanocomposite; Diamond-like carbon; Arc plasma.

1. Introduction

Mechanical seals assume critical significance as they influence the secure and efficient operation of rotating equipment, running and maintenance costs, energy efficiency, and environmental considerations across diverse industrial sectors. Mechanical seals [1] are vital for environmental protection by preventing gaseous and fluid leakage in machinery with rotating components. These seals are used in pumps, agitators, automotive engines, compressors, piston rings, shafts and bearings, heat exchangers, turbines etc. Their significance increases when working fluids pose risks due to toxicity, corrosiveness, flammability, or explosiveness. Common ceramic materials like silicon carbide (SiC), aluminium oxide (Al_2O_3), and graphite are employed for their high hardness, resistance to fatigue and corrosion, and low inertia [2, 3]. In alignment with the United Nations Sustainable Development Goals (SDGs), the exploration of advanced mechanical seals prioritizing their durability and sustainability is an active research area. The sustainability factor is now a key focus, aiming to make mechanical seals which have a long product life cycle, provide safe industrial operations, and uplift overall performance of rotating equipment while minimizing material leakage, and lower- energy consumption, costs, and environmental hazards [4, 5].

Despite extensive usage of SiC as a primary seal material, with notable properties such as high strength, low density, and excellent high-temperature resistance [6], its mechanical, tribological, and chemical properties have certain limitations. Achieving full densification of SiC involves intricate technology and requires very high sintering temperatures. Therefore, rendering the production of SiC ceramic material is costly and labour-intensive. Conventional methods of SiC fabrication result in simple structures, marked by low efficiency, high costs, and low yield, falling short of meeting engineering application requirements [7]. This challenge underscores the growing demand to extend the operation limits and overall lifespan of mechanical seals, prompting exploration into materials with superior mechanical, tribological, and chemical characteristics. Since the quest for high-performance SiC ceramic structures is still challenging, therefore, role of surface engineering and thin film coatings become significant to impart value-added characteristics to SiC substrates to advance their utility in critical engineering applications.

The performance of seals mainly relies on the mechanical and tribological characteristics of materials developing an interface contact. An emerging approach involves applying thin film coatings to enhance surface quality rather than relying solely on bulk material characteristics. Various coatings, including diamond, diamond-like carbon (DLC), graphite-like carbon (GLC), and carbide-derived carbon (CDC), have been explored [6]. These coatings are synthesised via chemical vapour deposition (CVD) techniques, e.g., hot filament CVD, microwave plasma CVD [8, 9] and physical vapour deposition (PVD) techniques such as magnetron sputtering, cathodic arc etc [10, 11]. Some literature reports propose CVD microcrystalline diamond film for mechanical seals [12, 13] as they have shown promising hardness and chemical resistance. Even though CVD diamond film exhibits high run-in friction coefficients during tribological tests due to the rough surface, which is attributed to large columnar grains, they have received preference over conventional diamond films. Despite promising mechanical seal applications, conventional diamond films require time-consuming polishing steps, rendering them impractical for commercial use [14]. An alternative approach involves synthesizing nanocrystalline [15] and ultra-nanocrystalline [12] CVD diamond films with smaller grain sizes, resulting in a smoother surface. However, fine-grain diamond films, such as nanocrystalline diamond, may exhibit high intrinsic stress, posing potential challenges to interface adhesion with the substrate [16]. Additionally, the use of substrate pre-treatment, diamond slurry for seeding purposes, gaseous precursors, and a thermal environment up to 800 °C are essential for diamond growth, which raises concerns over resources, altering substrate properties, environmental contamination by flue gases posing risk to the overall sustainability of product, process, and climate.

DLC coatings, an alternative carbon coating, exhibit hardness comparable to diamond, lower friction coefficients, cost-effectiveness, and environmental compatibility, especially when deposited via a PVD method in a vacuum with low substrate temperature [17]. However, the high compressive stress in DLC coatings can weaken the film-to-substrate bonding and limit the growth of thick coating [18]. Additionally, DLC coatings have a service temperature limit of 300 °C, with potential thermal degradation from SiC ceramics at 400 °C. Fu et al. [19] reported that C−H disbanding at a temperature beyond 500 °C leads to structural degradation of DLC coatings, causing a deterioration in DLC intrinsic characteristics. The humid environment particularly governs tribological performance in the context of DLC and SiC contact interface. The presence of water molecules at SiC-DLC interface forms additional bonds resulting in elevated friction coefficients [11]. To enhance the tribological performance of SiC ceramics, the unbalanced magnetron sputtering technique is also employed for depositing the GLC coating [20]. This coating exhibits an enriched composition of a graphite-like structure with high hardness attributed to interlocking of sp^2 bonds. Despite its promising tribological performance, observations of partial delamination between the GLC coating and the SiC substrate have been reported. Further, the DLC and GLC are recognised for lower deposition rates as compared to non-carbon coatings.

To achieve durability and sustainability in mechanical seals through coatings, the ideal coatings should exhibit reduced surface roughness and low coefficients of friction (CoF), resembling DLC and GLC coatings. Additionally, they should demonstrate wear resistance and appropriate thickness akin to diamond coatings while addressing the challenge of low adhesion to SiC ceramic seals. Considering these criteria, the impact of coating nanostructure and deposition methods on the durability of mechanical seals becomes paramount. Nanostructured materials like nanodiamond composite (NDC) films, amalgamating the advantages of diamond films and DLC [21-23], emerge as promising candidates for mechanical seal applications. NDC, a nanostructured carbon material comprising nanodiamond grains in an amorphous carbon matrix [24], exhibits extremely high hardness and Young's modulus, along with a smooth surface finish, complemented by impressive lower friction (CoF ≤ 0.1) and superior anti-wear properties [25-29].

Aligned with sustainable development goals [30-33], there is a growing emphasis on reducing energy consumption in coating synthesis, minimizing fabrication costs, and eliminating hazardous chemicals, lubricants, and coolants. Coaxial arc plasma deposition (CAPD) emerges as a favourable method for depositing NDC coatings on SiC mechanical seals. CAPD, an eco-friendly PVD technique, surpasses other methods by depositing NDC with lower internal stresses, tuneable morphology, and adjustable thickness at lower substrate temperatures up to 550 °C. Unlike CVD, CAPD avoids reactive gases, e.g., C_2H_2, CH_4, and H_2 [25, 34-36] which makes it versatile, and applicable to substrates without requiring a pretreatment process. CAPD is a clean and dry technique, devoid of hazardous materials, and waste generation, resulting in lower fabrication costs.

This research endeavours to augment the sustainability and durability of mechanical seals, particularly in environments with no external lubrication. Self-lubricating materials and dry friction conditions are of particular interest in these applications. To achieve this objective, an environment friendly NDC coating is applied on SiC ceramic substrates via the CAPD method, deliberately avoiding chemical gas reactions. A comprehensive evaluation of morphological, mechanical, and tribological properties is conducted on NDC-coated SiC materials. The aim is to elucidate the effectiveness of NDC coatings in extending the lifespan and enhancing the overall performance of SiC and to identify their potential for mechanical seal application.

2. Experimental details

2.1 Deposition of nanodiamond composite film

NDC films of approximate thickness of 1.1 µm were deposited onto silicon carbide (SiC) plates (20 × 20 × 3 mm) using CAPD equipment. **Fig. 1** illustrates the deposition process and experimental conditions to deposit NDC film on SiC substrate. The deposition process involved employing an arc plasma gun (ULVAC, APG-1000) with a 99.99% pure graphite rod (φ 10 × 22 mm) as the carbon source material to grow NDC film. A turbomolecular pump was used to produce a vacuum environment with pressure below 10^{-5} Pa. A substrate-to-target distance was maintained as 15 mm i.e., from the SiC substrate surface to the arc plasma gun. The arc gun facilitated the deposition process by operating at a voltage of 120 V with a repetition rate of 1.0 Hz and a capacitance of 720 µF, respectively. The substrates were cleaned with acetone and methanol for 5 minutes each before mounting into the chamber. Subsequently, following the evacuation process, a gradual substrate heating to 550 °C was implemented to enhance adhesion.

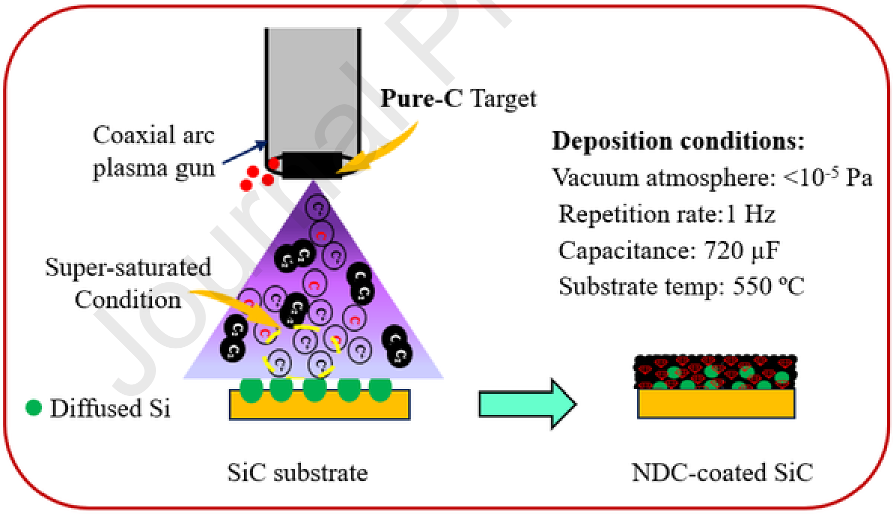

Fig. 1. Schematic of coaxial arc plasma deposition process and experimental conditions to deposit nanodiamond composite (NDC) film on silicon carbide (SiC) substrate

2.2 Characterization of nanodiamond composite film

2.2.1 Morphology studies

The morphology of as-deposited films was investigated using field emission scanning electron microscopy (FE-SEM) for a plane view and a cross-sectional view, respectively. Elemental composition was in situ analysed using an Energy Dispersive X-ray Spectroscopy

(EDS) system integrated with FE-SEM (JEOL, JSM-IT700HR). Surface roughness, characterized by arithmetic mean height (Sa) in a specific area of 129 μm × 130 μm and average roughness (Ra) across an 80 μm length, were measured using a 3D laser microscope (LEXT OLS5000, Olympus, JP). Raman spectra were obtained using a Lambda Vision Raman system (MicroRAM-300ATG(KS)) with a confocal microscope (in Via, Renishaw) and a high-performance CCD detector. The laser power was maintained at approximately 30 mW, and a neutral density filter was employed to attenuate the laser intensity. A conservative 5% of the laser power, with a spot diameter of ≤ 1 μm, was applied during sample detection. The Raman scattering range was covered from 100 cm^{-1} to 3600 cm^{-1}, and calibration of the wavenumber axis was performed using a Si (001) peak at 520.6 cm^{-1}.

2.2.2 Mechanical testing

The nanoindentation platform (Picodentor HM500, Fischer Instrumentation, UK) equipped with a Berkovich diamond tip was used to assess the hardness and Young's modulus of NDC films. To ensure reliability, measurements were conducted at ten different points across the sample, with the maximum indentation depth carefully controlled below 10% of the film thickness to mitigate the substrate influence [37, 38]. The testing parameters comprised a maximum load of 5.0 mN, a loading rate of 5.0 mN/10 s, and a dwell time of 5 s. Additionally, scratch adhesion testing was performed with a diamond-tipped Rockwell N2–6266 indenter over a 5 mm scratch length, and the critical load was determined through optical microscopy of the scratched track. The assessment of adhesion between the SiC substrate and the NDC coating involved Rockwell indentation tests with ascending loads of 60, 100, and 150 kg which corresponds to 588, 980, and 1470 N, respectively.

2.2.3 Tribological testing

The tribological performance of the NDC films was investigated at room temperature using a ball-on-disk tribometer, with a SiC ball (ϕ 2 mm) as a counterpart under dry sliding conditions. A comprehensive tribological study aimed to assess the coating behaviour in harsh environmental conditions, with a particular emphasis on the coatings' suitability for eco-friendly mechanical seal applications. Therefore, the applied load, air humidity, and sliding speed were set at 2.94 N, 50%, and 0.2 m/s, respectively. To control the effects of surface dissipation energy, the wear track radii of 7±1 mm and sliding duration of 10, 30, and 60 min were configured. Following the friction tests, the wear track width and wear rate of the counterpart were calculated in worn volume, area, and depth using the 3D laser microscope. The wear rate of the films was calculated according to the Archard equation

[39]: $k = \frac{V}{F \times L}$, where k denotes the wear rate (mm^3/N·m), V denotes the wear volume (mm^3), F denotes the normal load (N), and L denotes the total sliding distance (m).

3. Results and discussion

3.1 Surface morphology and structural analysis of NDC film

Referring to **Fig. 2**, the resulting NDC coatings displayed a dense structure with a uniform, smooth, and relatively flat surface, measuring a thickness of 1.1 µm. The high deposition rate of 0.73 nm/pulse reflects the better efficiency of the CAPD process over typical CVD/PVD methods. Both, plane (**Fig. 2a**) and cross-sectional (**Fig. 2b**) SEM images confirmed the uniformity and dense structure of the NDC film, where a granular morphology of NDC could be observed in the high-resolution inset image of **Fig. 2a**.

Selecting the optimal film thickness is crucial for balancing performance and cost. While thicker films might seem ideal, they can be more expensive to produce. Conversely, thinner films can be more cost-effective while still delivering good tribological properties [40]. Based on similar studies [41, 42], a thickness of ≥ 1 µm was chosen for the NDC film for several reasons. First, it strikes a balance between performance and cost-effectiveness. Second, it ensures the film is thick enough to eliminate the influence of the substrate on nanoindentation measurements. Third, it allows for a dense film to be deposited by exceeding the thickness of the interfacial layer (around 300 nm). Finally, it minimizes the risk of delamination by limiting the buildup of compressive stress within the film.

Three-dimensional surface profiles were obtained using a 3D laser confocal microscope to analyze the texture of the SiC substrate and the deposited NDC film (**Fig. 2c** and **Fig. 2d**). Optical profilometry revealed a relatively smooth film surface with consistent average roughness (Ra) of 60 nm and area roughness (Sa) of 80 ± 5 nm. However, high-resolution SEM revealed additional details not captured by these average roughness parameters. High-magnification SEM images (**Fig. 2a** inset) highlighted the presence of nanoscale, clustered grains with a spherical morphology (scale bar = 1 µm). These features correspond to the red asperities observed in the 3D profile of the NDC film (**Fig. 2c**). The 3D profile further differentiates the film and substrate based on their height variations, represented by distinct color zones (yellow and green for the substrate, red, yellow, and green for the film).

While the average roughness parameters (Ra and Sa) suggest minimal variation between the film and the substrate, it's crucial to consider the limitations of these metrics.

They primarily capture the average height deviation from a reference plane and might not fully represent the presence of localized features. Peak-to-valley height (Sz) and ten-point height (Rz) offer a more comprehensive characterization by considering the extreme height variations on the surface. These parameters increased significantly (Sz from 1.3 µm to 2.39 µm and Rz from 0.4 µm to 0.49 µm) after NDC deposition (**Fig. 2e**). This observation aligns with the visual cues from the 3D profile, suggesting the introduction of surface features with larger height variations on the film compared to the substrate, despite the similar average roughness values.

This observation suggests that the initial roughness of the substrate played a key role in determining the final surface roughness of the coating. This aligns with previous research on the growth of CVD nanocrystalline diamond (NCD) deposited on SiC substrate [15]. The NCD films exhibited same surface roughness of SiC substrate. This suggests that the preparation of both NDC and NCD did not significantly alter the surface roughness of the SiC seal.

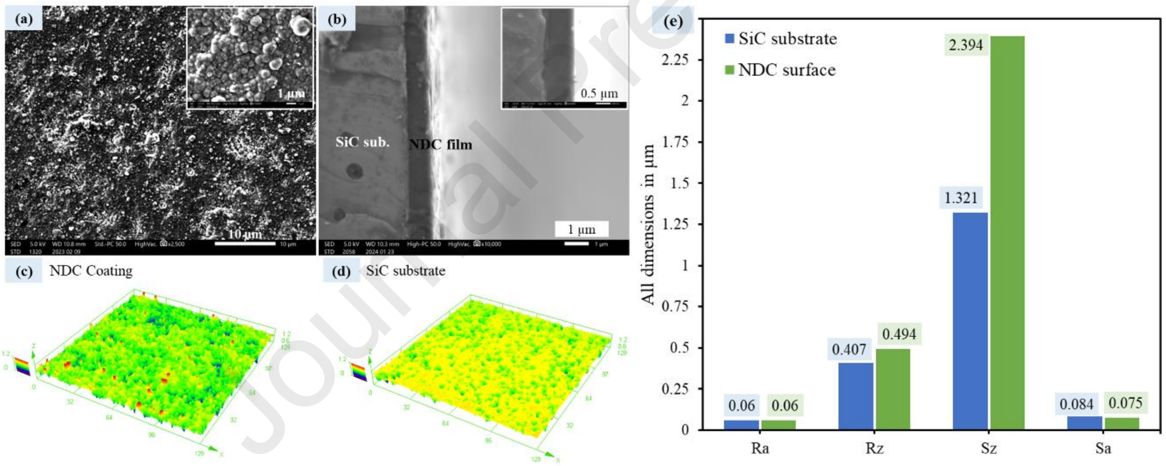

Fig. 2. FE-SEM micrographs of NDC film: (a) plane view and (b) cross-section view, along with 3D surface topography of (c) NDC film and (d) SiC substrate, and (e) summary of surface roughness parameters.

The significance of initial surface roughness on the tribological properties of SiC-based seals has been emphasized in previous literature [43]. Maintaining smooth surfaces is crucial to prevent high friction and severe wear on the seal articulating surface, ultimately avoiding rapid and premature seal failure [44, 45]. While comparing the roughness of NDC with conventional microcrystalline diamond films [46], NDC coatings exhibit a smoother surface with a roughness of 60 nm as compared to 300 nm roughness of conventional microcrystalline diamond films and this is attributed to the smoother SiC substrate surface.

Additionally, NDC coatings can be deposited at a lower temperature of 550 °C when compared to conventional microcrystalline diamond films which are typically deposited at 800 °C. A relatively lower temperature prevents changes in substrate physical and chemical compositions and can grow a film in a vacuum atmosphere without hazardous chemical reactions during deposition. This underscores the effectiveness of CAPD in fabricating eco-friendly and smooth hard carbon films for SiC seal applications.

Visible Raman analysis was conducted to elucidate the intricated structural characteristics of the NDC coatings, providing valuable insights into their physical origins and tailored properties. The Raman spectra, meticulously collected from surface of the as-deposited coating, are illustrated in **Fig. 3** and reveal four distinct broad bands spanning the ranges of 200 ~ 700 cm^{-1}, 700 ~ 1,000 cm^{-1}, 1,000 ~ 1,600 cm^{-1}, and 2,000 ~ 3,500 cm^{-1}.

In the first band (200–600 cm^{-1}), the activation of Raman modes related to acoustic phonons of amorphous silicon carbide (a-SiC) [47, 48] or amorphous silicon (a-Si) [49], or a combination of both [50] were observed. The second band (700 ~ 1000 cm^{-1}) exhibited specific SiC peaks, including transverse optical (TO) and longitudinal optical (LO) modes at around 790 cm^{-1} and 960 cm^{-1} [51], indicating structural disorder in SiC bonds attributed to the optical Raman modes of amorphous SiC (a-SiC).

Moving to the third band (1,000 ~ 1,600 cm^{-1}), the Raman spectrum displayed characteristic features of NDC consistent with those of ultra-nanocrystalline diamond (UNCD) [12] and nanocrystalline diamond (NCD) [15] films deposited on SiC ceramics. Peaks at 1333 cm^{-1} and 1580 cm^{-1}, along with t-PA_1 and t-PA_2 shoulders at 1170 cm^{-1} and 1464 cm^{-1}, respectively, indicate the presence of a nanodiamond phase with abundant grain boundaries (GBs). The overlap at 1333 cm^{-1} between the first-order diamond peak and D-peak highlighted the mechanical properties contributed by the C–C sp^3 bonding, while the D-peak suggested the presence of amorphous/graphitic carbons at the grain boundaries, influencing tribological properties [52, 53]. The G-peak at 1580 cm^{-1} represented the in-plane (E2g) stretching mode of C=C sp^2 bonds in both rings and chains of the amorphous graphitic phase [54].

To delve into the nanostructure composition of NDC coatings, we conducted deconvolution on the Raman spectra of the third band, as illustrated in **Fig. 3** (Onset). Six peaks emerged, with a distinctive one near the natural diamond Raman peak (1332 cm^{-1}), confirming the presence of diamond grains. The characteristic Raman peak of sp^3 diamond at 1333 cm^{-1} indicated the existence of nanodiamonds, attributed to highly energetic C^+ species within the CAPD plasma. Peaks at 1170 cm^{-1} (t-PA_1) and 1464 cm^{-1} (t-PA_2)

validated the presence of abundant grain boundaries (GBs) due to the formation of the nanodiamond phase. This phase is associated with the stretching of C=C sp^2 and the wagging of C−H modes in trans-polyacetylene chains. These outcomes affirm the prevalence of nanodiamond grains within an amorphous carbon (a-C) matrix, forming numerous grain boundaries that fortify film strength while concurrently mitigating internal stress, characterizing the NDC material as a nanostructured nanocomposite.

Furthermore, the emergence of the G band (around 1580 cm^{-1}) in the Raman spectra indicated the development of graphite-like sp^2 bonded carbon within the grain boundaries of the NDC coating. The G-peak bifurcated into G_1 at 1553 cm^{-1} and G_2 at 1596 cm^{-1}, representing the in-plane stretching mode of C=C sp^2 bonds in both rings and chains of the amorphous graphitic phase. It was reported that, the G-peak is typically identified within the range of 1510 to 1580 cm^{-1} (G_1-peak). Additionally, this range may extend to approximately 1600 cm^{-1} (G_2-peak), emphasising the presence of a high fraction of sp^3 chains [55, 56]. The presence of the G_1 and G_2 peaks suggests a chain-dense tetrahedral amorphous carbon structure and an amorphous diamond structure, respectively, contributing to the improvement of the mechanical and tribological properties of the NDC film. The appearance of the D-band at a Raman shift of ~1345 cm^{-1} corresponds to the disorder-activated aromatic mode of A1g symmetry [57]. In the NDC film, the D-peak at 1345 cm^{-1} concurred with observations reported in studies on nanocrystalline diamond [58]. This alignment reflects the impact of nanodiamond presence, contributing to the reduction of defects and enhancing films properties.

The fourth band (2,000 ~ 3,500 cm^{-1}) corresponds to the second-order Raman scattering revealing a weakly structured with a broad band within a range of 2,500 ~ 3,200 cm^{-1}, which is attributed to second-order Raman scattering of disordered graphite. This included a mixture of overtones of the D-and G-peaks modes and their combinations [59]. The Raman spectrum within this band exhibited the characteristic 2D band at 2,680 cm^{-1} and (D+G) band at 2,900 cm^{-1}, along with weak lines at 2,260 and 2,590 cm^{-1} attributed to the second-order Raman scattering of trans-polyacetylene (t-PA) modes [60]. These findings align with observations in the second-order Raman scattering of nanocrystalline diamond film modes [61]. This observation serves as additional evidence supporting the nanostructure composition of NDC coating, indicating the presence of a nanodiamond phase embedded in a-C matrix.

Furthermore, Raman analysis of the as-deposited NDC coating on SiC substrate not only revealed the nanostructure composition of the coatings but also exhibited the characteristic peaks associated with the formation of intermetallic compounds (SiC) within the film. This phenomenon releases internal stress in the films and enhances adhesion to the substrate. The highly energetic C^+ species within the CAPD plasma reached the substrate surface, initiating the diffusion of Silicon (Si) from the substrate. This results in the formation of stable Si–C *sp³* bonds, contributing to the films' hardness and adhesion. Remarkably, the Si−C bonds are longer than C−C bonds, alleviating internal stress in films [27]. This comprehensive Raman analysis contributes to a deep understanding of the intricate structural features and composition of the NDC films, shedding light on their potential applications in SiC-based mechanical seals.

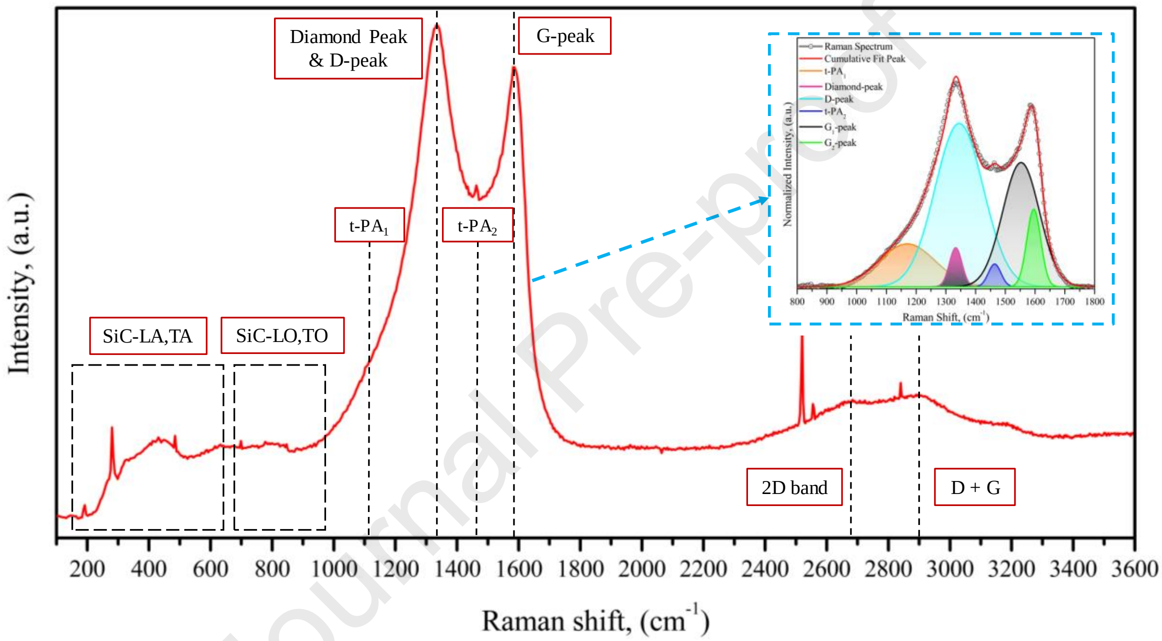

Fig. 3. Raman spectrum of the as-deposited nanodiamond composite film on silicon carbide substrate, demonstrating the characteristic peaks of nanostructure composition of the film.

3.2 Mechanical properties of nanodiamond composite film

3.2.1 Nanoindentation results

The nanoindentation measurements were conducted on ten randomly chosen locations on the surface of the NDC film and compared to the substrate. The measured hardness and elastic modulus of the SiC substrate were 53.3 GPa and 572 GPa, respectively. These values are consistent with recent research findings [62, 63]. The NDC coating exhibited a notable hardness (H) of 48.5 GPa with an 8% variation and a Young's modulus (E) of 496.7 GPa with an 11% variation (**Fig. 4)**. It is acknowledged that the NDC coating exhibits a slightly lower hardness compared to the SiC substrate (approximately 5 GPa difference). However, the unique structure of the NDC coating, consisting of nanodiamond grains embedded within an a-C matrix, offers significant advantages in terms of tribological performance. In dry sliding conditions, the solid-solid contact between ceramics and the mating test balls typically results in high friction due to the absence of effective lubrication. The NDC coating addresses this challenge by functioning a lubricating film at the contact interface, as will be elaborated upon in the following section.

The load-displacement curves were further analysed to estimate various elastic and plastic properties of the films. The observed variation in hardness measured at 5 mN for NDC films, indicates a strong correlation with the nano- to micro-structural defects within the network. This correlation is intricately linked to the bonding between atoms and their ability to withstand deformation arising from compression, volumetric expansion, bending, or breaking. Concurrently, Young's modulus (E) is contingent on the slope of the harmonic interatomic potential.

Furthermore, the plasticity index (H/E = 0.098) and enhanced fracture toughness (H^3/E^2 = 0.46 GPa) are attributed to the effects of plasma properties, characterised by highly energetic C^+ ions. The plastic resistance index (H/E) not only elucidates elastic–plastic characteristics but also provides insights into wear resistance. The H/E ratio signifies the physical response of an atomic lattice to an external force and correlates with bulk fracture strength. The observed H/E (0.098) in the NDC film corresponds to lesser plastic deformation, implying higher wear resistance and, consequently, a more diamond-like character. Notably, natural diamond with H ≈ 100 GPa and E ≈ 1000 GPa, exhibits an H/E ratio of ≈ 0.1. The improved H/E parameter of 0.098 promotes NDC coatings for durable and anti-wear applications.

Elastic recovery (R) was calculated using the formula $R = (h_{max} - h_{res})/h_{max}$ [64], where h_{max} and h_{res} are the maximum displacement at peak load during loading and residual displacement after unloading in a nanoindentation cycle.

A high value of elastic recovery (R = 0.75) was observed for the NDC coating, consistent with the elastic recovery of CVD diamond [65, 66]. Therefore, NDC films not only prove suitable for hard and protective applications but also exhibit potential in high-wear-resistance coating applications. The subsequent section will provide a detailed discussion of the films' wear resistance.

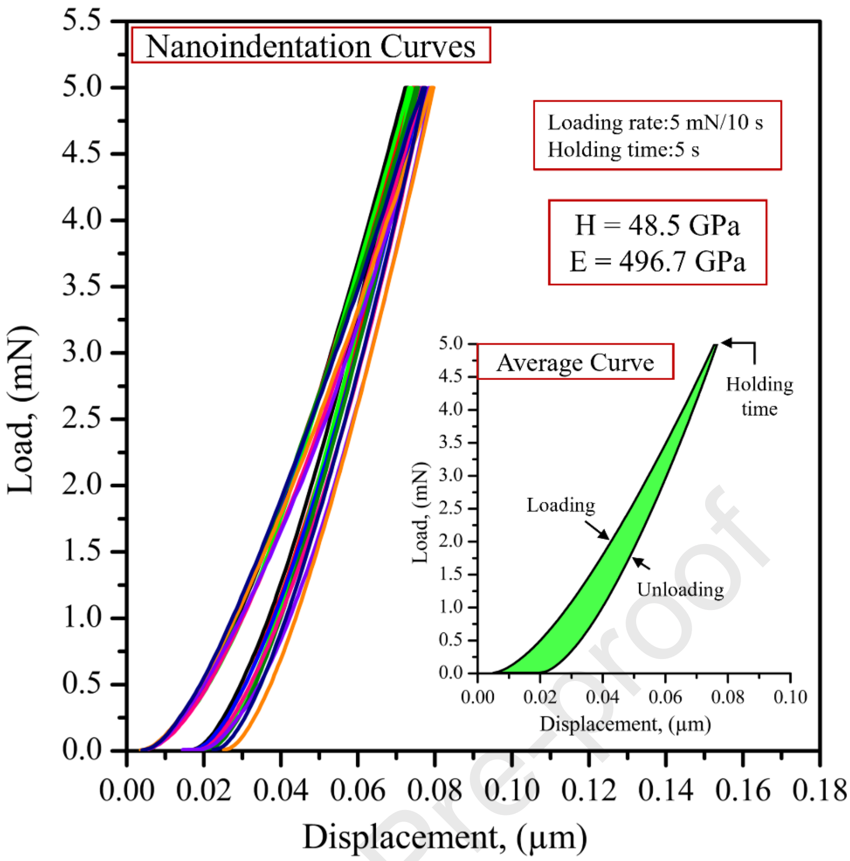

Fig. 4. Nanoindentation test results and mean load-displacement curves of nanodiamond composite film deposited on silicon carbide substrate.

3.2.2 Adhesion studies of nanodiamond composite film

Adhesion studies were performed with scratch test and Rockwell hardness tester. The scratch test method [25] as illustrated in **Fig. 5a**, provides a practical approach for evaluating the adhesion properties of a thin, hard coating to its substrate [67, 68]. Employing a Rockwell diamond-tipped indenter with a normal load ranging from 1 N to 60 N and a load rate of 120 N/min, a 5 mm scratch length was traversed on the sample. The plot shows acoustic emission, tangential force, and friction coefficient against progressively increasing normal loads during the scratch test. Coating delamination, indicated by a sharp rise in acoustic emission, tangential force, and friction coefficient due to elastic energy release, allows for the assessment of the critical load [69, 70]. The absence of any peak in the acoustic emission signal within the load range for the NDC coating, indicates that no film delamination occurred which was also cross-checked with optical microscopy as shown in **Fig. 5b** and **c**.

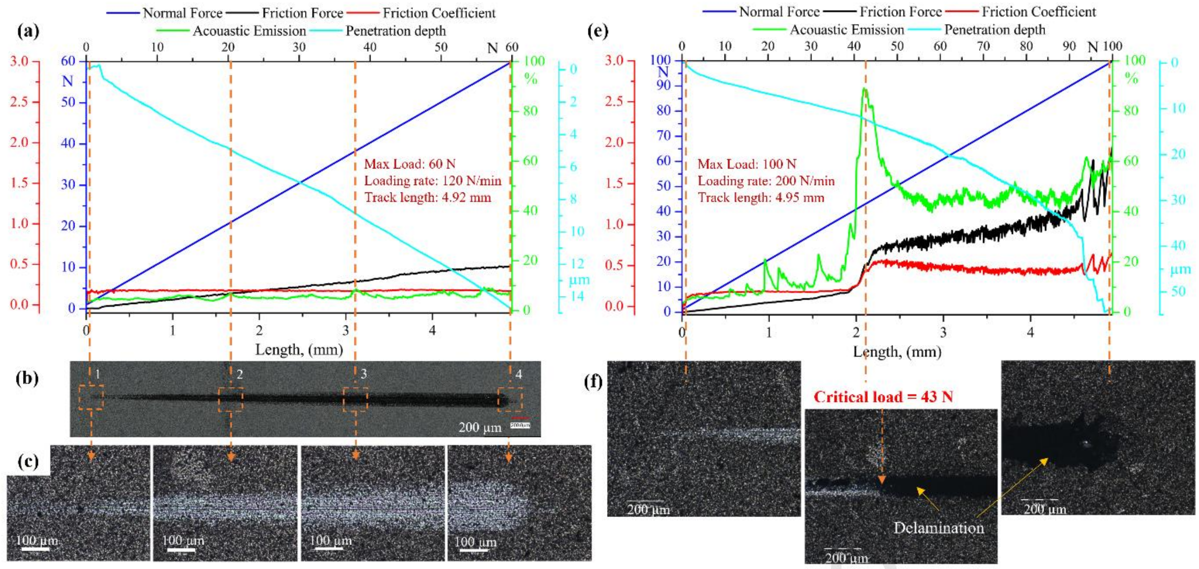

Fig. 5. Scratch tests of NDC films at loads of (a) 60 N and (e)100 N, (b, f) Optical images of the entire 5 mm scratch at each load, (c) High-resolution images of specific scratch positions (1-4) at 60 N load.

Furthermore, with increasing loads as observed at various points (1, 2, 3, and 4), no debris or chipping is observed along the scratch tracks. Additionally, there is no delamination of film observed in the vicinity of these locations, as depicted in **Fig. 5b** and **Fig. 5c**.

To further challenge the film adhesion, a second scratch test was conducted with a modified protocol: a higher normal load range (1 N to 100 N) and a faster load rate (200 N/min) (**Fig. 5a**). In this test, critical load for delamination was monitored through acoustic emission, tangential force, and friction coefficient measurements (**Fig. 5e**). A rapid increase in these parameters indicates the dissipation of elastic energy during a coating breakdown event. Notably, a distinct peak in the acoustic emission signal was observed at a normal load of 43 N for the NDC film (**Fig. 5f**), signifying the critical load for delamination under these more aggressive test conditions.

This observation suggests that the NDC film exhibits superior scratch resistance, attributed to potentially lower compressive internal stresses, the formation of intermetallic compounds (SiC) within the film and particularly at the interface. Consequently, the application of NDC film holds the potential to enhance the mechanical performance and durability of SiC for mechanical seal applications.

Rockwell indentation tests were conducted to gain a comprehensive understanding of film adhesion and assess the toughness of the NDC film. **Fig. 6** presents the optical images of indentation craters produced by Rockwell tester on NDC film. Observations reveal coating cracks and spallation, as evidenced by tiny annular cracks around the imprint. However, it could be observed that the coating still remained adherent to the substrate. These characteristics can be attributed to the brittle nature of the SiC substrate. This outcome signifies an enhanced adhesion between the NDC coating and the substrate.

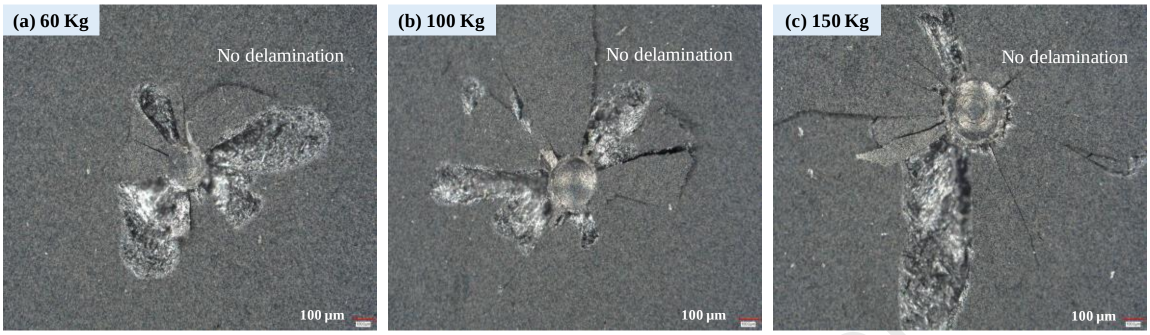

Fig. 6. Optical images illustrating the indentation crack morphology due to Rockwell testing of the nanodiamond composite film under various loads.

The scratch and indentation testing reveals a noteworthy improvement in film adhesion to the substrate and justifies the potential of NDC coating for mechanical seal applications, particularly when NDC films remain adherent till a critical load (L_{cr}) of 60 N. This improvement is influenced by several crucial factors. The diffusion of Si atoms at elevated substrate temperatures facilitates the formation of stable intermetallic compounds, such as silicon-carbide (SiC), at the interface. This observation is consistent with findings from our previous work when NDC coatings were deposited on a Si substrate at a similar substrate temperature [52]. It is perceived that CAPD process significantly contributes to the growth of strongly adherent films.

To gain insights into the composition of the films, EDS mapping of a top view and cross-sectional view (across interface) along with the depth profiles and EDS spectra were measured, as presented in **Fig. 7**. The NDC film is mainly composed of C elements, with observable and detectable small amounts of Si atoms diffused from the substrate into the film, forming Si−C bonding as detected by Raman analysis. Notably, at the interface, a more intense Si spectrum is detected, indicating the presence of Si, contributing to the formation of an interfacial layer containing SiC intermetallic. This underscores the success of NDC interactions with the substrate elements at the interface, ultimately fostering the development of a highly adherent NDC film onto the SiC ceramic substrate.

For NDC coatings, the successful deposition of durable and hard films with strong adhesion relies on the presence of nanodiamond grains introducing large numbers of GBs, which release internal stresses due to GBs and Si−C formation within the film, and corresponding interactions occurring at the film-substrate interface. A comprehensive understanding of these factors with systematic experimental design and computation methods is crucial for optimizing the performance of NDC coatings in mechanical seal applications.

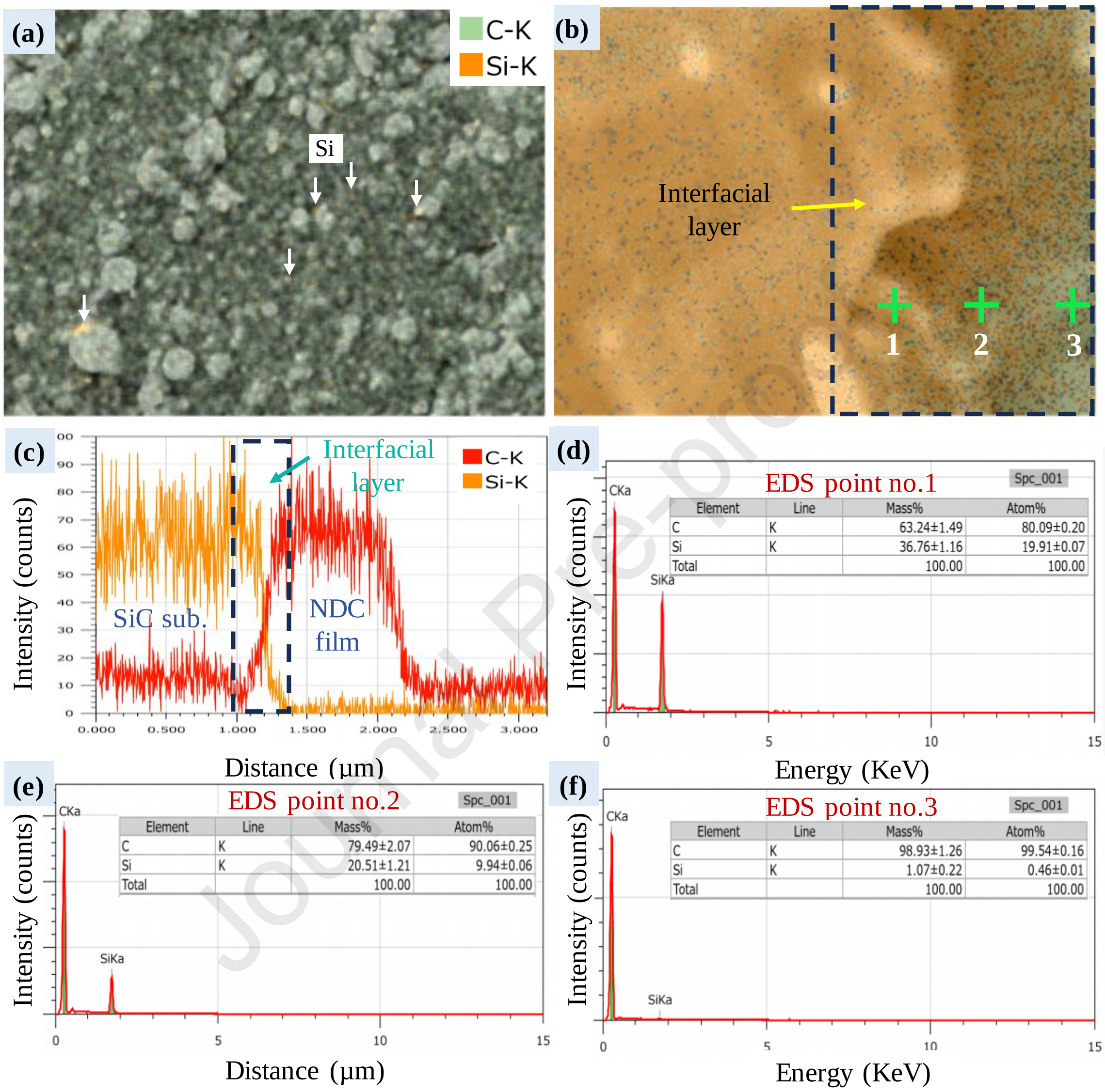

Fig. 7. (a) Plane view and (b) cross-sectional EDS mapping of the NDC film, complemented by (c) cross-sectional depth profile elemental scanning, and (d, e, and f) corresponds EDS spectra at points no. 1, 2, and 3 through the interface marked in (b).

3.3 Tribological performance of nanodiamond composite film

In the context of contemporary industries, there is a pressing demand for materials that have a good combination of enhanced wear resistance with low coefficients of friction to prolong the operational lifespan of mechanical components and mitigate energy losses. Traditional methods for enhancing wear resistance capabilities typically involve reinforcing both hardness and toughness. A promising approach involves constructing a nanocomposite structure, integrating numerous nanodiamond grains within an amorphous carbon matrix. This strategy simultaneously enhances hardness and toughness by impeding dislocation across interfaces and deflecting interface-induced micro-cracks [71, 72]. Such advanced materials find crucial applications in diverse industries, particularly in mechanical seal applications, where wear resistance and low friction coefficients are paramount for ensuring machinery longevity and efficiency.

The tribological behaviour of the SiC substrate with and without NDC films was compared using a ball-on-disc tribometer under ambient conditions (dry sliding in air). The results, presented in **Fig. 8a**, show a significantly lower friction coefficient for the NDC-coated SiC (around 0.15) compared to the bare substrate (around 1.22) after 30 minutes of sliding.

Fig. 8b reveals a characteristic initial peak in the friction trace for both samples. This peak is attributed to the initial interaction and interlocking of asperities (rough surface peaks) on the contacting surfaces [73]. As sliding progresses, these asperities wear down, leading to a smoother contact interface and a decrease in friction observed in the latter stages of the test.

The influence of sliding duration on wear is further explored in **Fig. 8c** and **8d**. **Fig. 8c** shows the friction curves for the NDC film and the corresponding wear rate of the SiC counter-body for sliding times of 10, 30, and 60 minutes. **Fig. 8d** summarizes the average CoF and wear rates for the counter-body. The CoF values increase slightly from 0.12 to 0.18 with increasing sliding time, while the wear rate of the counter-body exhibits a similar trend (2.78 x 10^-7 mm^3/N·m to 3.91 x 10^-7 mm^3/N·m). These results suggest that the wear behaviour of the system evolves with sliding duration.

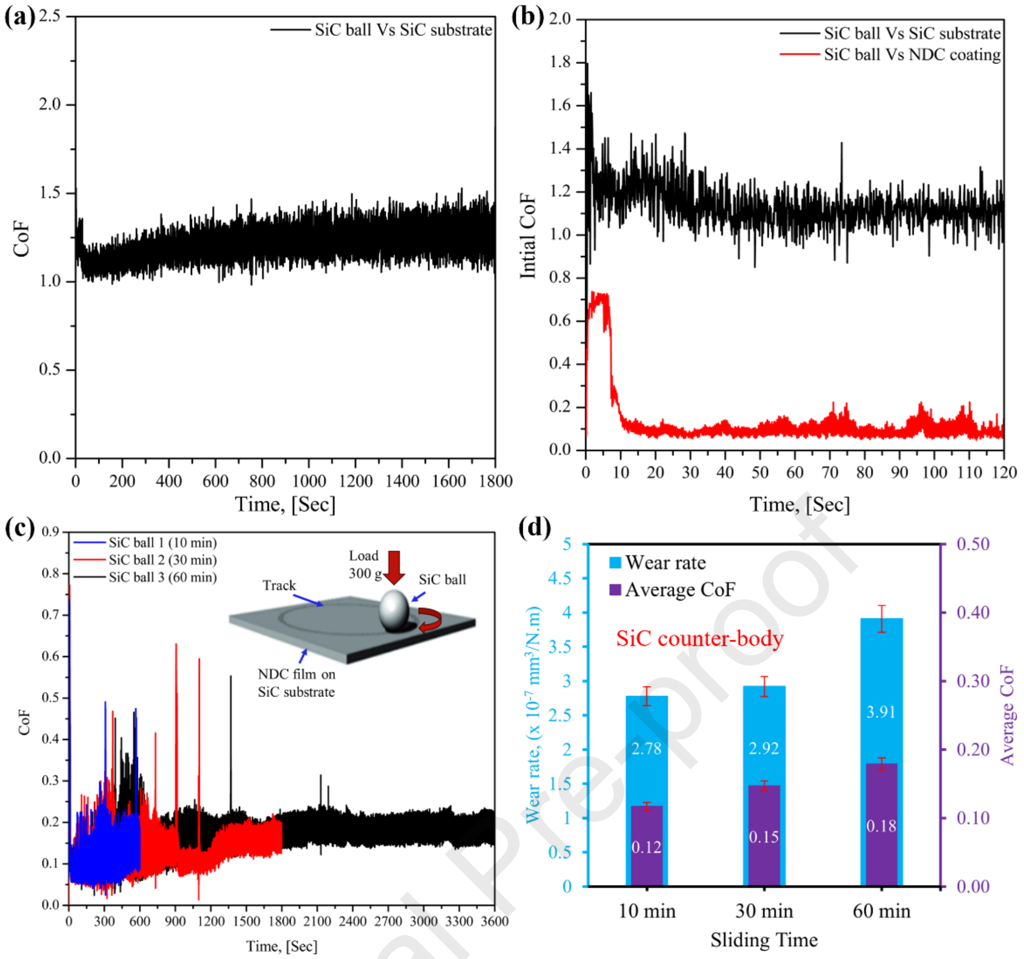

Fig. 8. NDC film tribology in ambient air: (a) SiC substrate friction, (b) Initial CoF, (c) Friction vs. time, (d) CoF and wear rate of SiC counter-body.

The CoF profile of the NDC film is categorized into three regions: initial running-in, transition, and steady state. Initially, the NDC sample displays a higher CoF, attributed to surface roughness and the presence of asperities, as indicated in the three-dimensional profile taken by a 3D laser confocal microscope. As sliding progress, sharp asperities wear down, and valleys fill with micro-fractures and debris, leading to smoother interfaces. The resulting friction curves exhibit noticeable fluctuations during the initial running-in and transition stages, suggesting wear of the SiC counter-body due to Si content compared to the NDC coating. Additionally, the presence of asperities on the NDC film surface exerts concentrated contact stresses, further contributing to an increased wear rate in the SiC counter-body. The observed fluctuations in the CoF profile are indicative of the dynamic interactions between the SiC counter-body and the NDC film during different stages of the sliding process until reaching the steady state, emphasizing the evolving tribological characteristics of the system.

The tribological performance of NDC films is revealed through the formation of a stable and protective tribolayer after around 20 minutes of sliding. This tribolayer's creation is facilitated by the abundance of grain boundaries within the NDC film and the high contact pressure during sliding. These factors promote the rehybridization of carbon atoms from a diamond-like structure (sp^3 bonding) to a more lubricant graphite-like structure (sp^2 bonding) [74]. This tribolayer acts as a solid lubricant, reducing friction and wear on the NDC film. Additionally, the diffusion of silicon atoms from the underlying SiC substrate into the film aids in stabilizing the coefficient of friction.

The low friction coefficient of NDC films can be attributed to a combination of mechanisms. Raman spectroscopy (**Fig. 9a**) reveals a key transformation: during the test, the carbon atoms within the film rearrange into a more lubricating, graphite-like structure (confirmed by the increased intensity of the G-band compared to the D-band and diamond band compared with those before the test in **Fig. 3**). This process, known as graphitization, likely leads to the formation of a lubricating film at the real area of contact between the surfaces. Additionally, the possibility exists that a separate lubricating film might also be transferred to the opposing SiC counter-body during sliding [75].

Furthermore, the ambient environment, specifically the presence of oxygen and water vapor in the air, plays a crucial role [76]. These molecules interact with the sliding surfaces, effectively weakening the adhesion between them. This translates to weaker van der Waals forces, ultimately contributing to the exceptionally low coefficient of friction observed in NDC films. In essence, the combination of a potentially self-generated lubricating film, a possible transfer film on the counter-body, and reduced adhesion due to the ambient environment all work together to achieve the low friction properties that make NDC films so promising for wear-resistant seals.

Simultaneously, the debris generated during the sliding process serves as a third body between the film and the counter-body, exerting additional influence on the CoF. These debris accelerate the formation of grooves in the SiC counter-body, leading to an increase in surface roughness over sliding time as summarized in **Fig. 9b**. In contrast, the NDC film exhibits a smoother surface with increasing sliding time due to the fracture of the asperities along with extended sliding time. Consequently, the asperities significantly contribute to a higher wear rate in the counter-body compared to the NDC films.

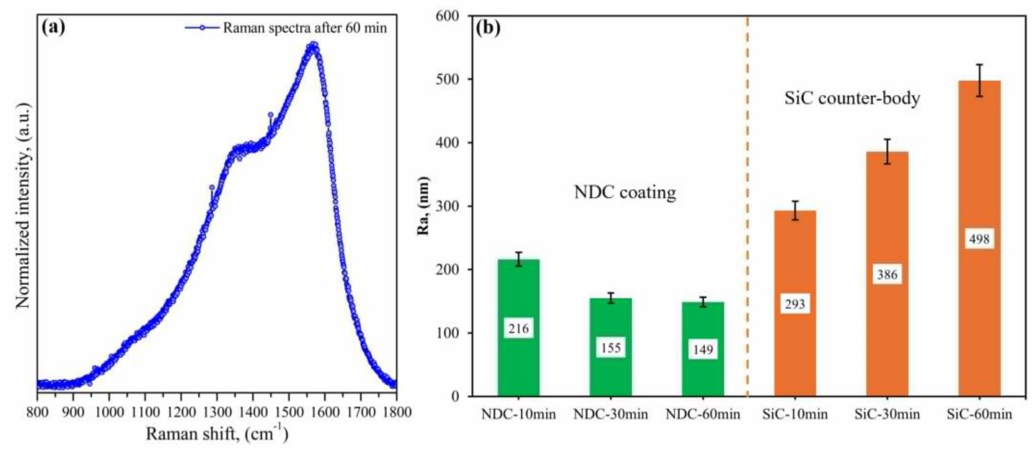

Fig. 9. (a) Raman spectra of NDC coating after friction test (Sliding time = 60 min) and (b) Surface roughness of NDC film and SiC counter-body after a pin-on-disc test at 300 g normal load, 0.20 m/s velocity, for a duration of 10, 30, and 60 min of dry sliding under ambient conditions.

The Hertz model for a sphere on a flat surface [77] was employed to calculate the maximum contact pressure experienced during the tribological test. Considering a spherical contact between the SiC ball (diameter of 2 mm) and the NDC film, the analysis revealed a maximum contact pressure of approximately 3.1 GPa at a depth of ~21 μm. While this pressure is deeper than the thickness of the NDC films (1.1 μm), it's important to note that it's concentrated within a limited zone. This suggests a lower contact pressure at the crucial interface between the film and the substrate. This observation aligns with the strong interfacial bonding evident in the microstructure analysis (**Fig. 5**) and scratch tests (**Fig. 7**). The robust interface effectively hinders crack initiation and growth under load, promoting good film adhesion. Therefore, the NDC films demonstrate potential for application in real-world mechanical seals, where even higher contact pressures (up to 1000 psi or more) are encountered [78, 79].

Wear resistance was assessed by estimating the depth and area of wear tracks to calculate the wear volume of SiC counter-body, as illustrated in **Fig. 10** and summarized in **Fig. 11**. These factors were indicative of the wear performance observed during the friction test. Surface profiles of corresponding wear tracks, as depicted in **Fig. 12**, were analysed to further assess the wear resistance of the NDC films against SiC counter-body. The SiC counter-body exhibited a gradual increase in wear with increasing test time. These values were found to be in line with the track width in the NDC films, which increased for longer sliding periods, coupled with a growing worn area on SiC counter-body during the friction test. After sliding a distance of 720 m at the maximum duration of 60 min, the recorded parameters for wear of SiC ball were as follows: a worn volume of 844,815 µm³, an area of 119,227 µm², a depth of 15.6 µm, and a corresponding track width of 302 µm.

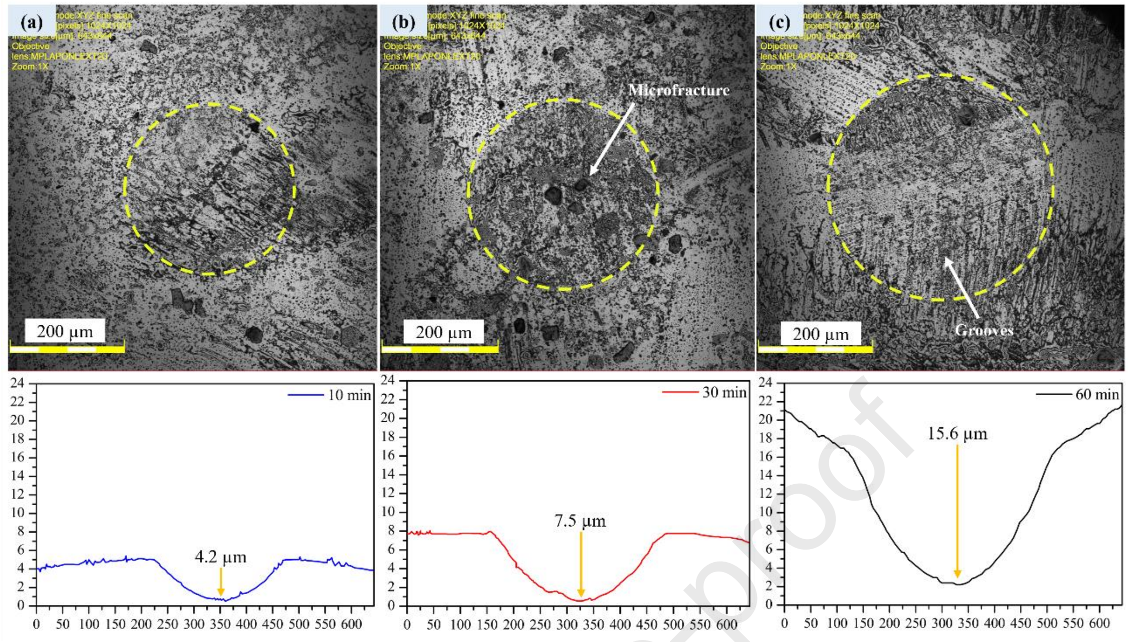

Fig. 10. 3D scanning of wear scar on SiC counter-body after friction/wear tests at different sliding periods, along with depth profiles.

This study demonstrates that NDC coatings hold significant promise for surpassing existing seal materials in terms of low friction and wear resistance. Compared to commonly used coatings like diamond, diamond-like carbon (GLC), carbon doped chromium (CDC), and even silicon carbide coatings (SiC), NDC coatings exhibit promising performance, as detailed in Table 1.

The exceptional wear resistance of NDC-coated SiC is particularly relevant for mechanical seal applications. Analysis of the wear track on NDC films after testing reveals a remarkably smooth surface with minimal wear, even after extended periods of sliding. Additionally, wear track profiles measured perpendicular to the rotational direction show no significant change compared to the unworn surface, confirming the absence of linear wear. This exceptional performance extends even under harsh conditions: no delamination of the NDC films was observed after a 1-hour run-in period without lubrication.

The outstanding anti-wear properties of NDC coatings are attributed to their superior self-lubricating ability when interacting with the SiC counter-body. This self-lubricating characteristic is further supported by the unchanged steady CoF curve, especially during extended testing durations. These findings suggest that NDC coatings offer a promising solution for enhancing the durability and wear resistance of SiC seals in demanding applications.

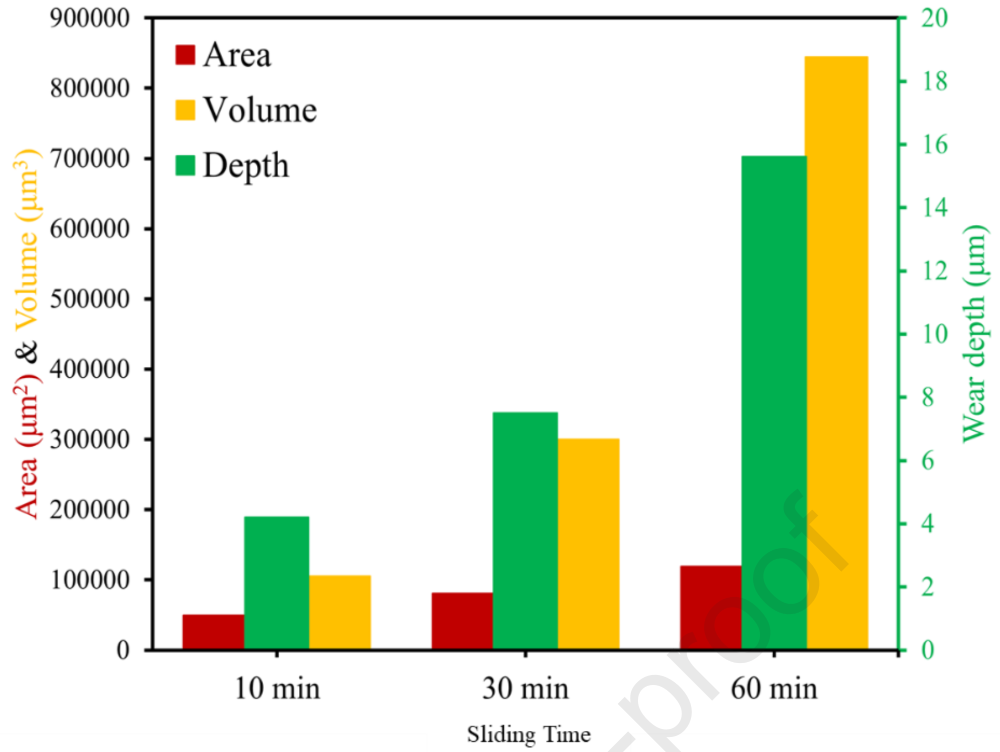

Fig. 11. Wear assessment of silicon carbide counter-body against nanodiamond composite film at different sliding durations

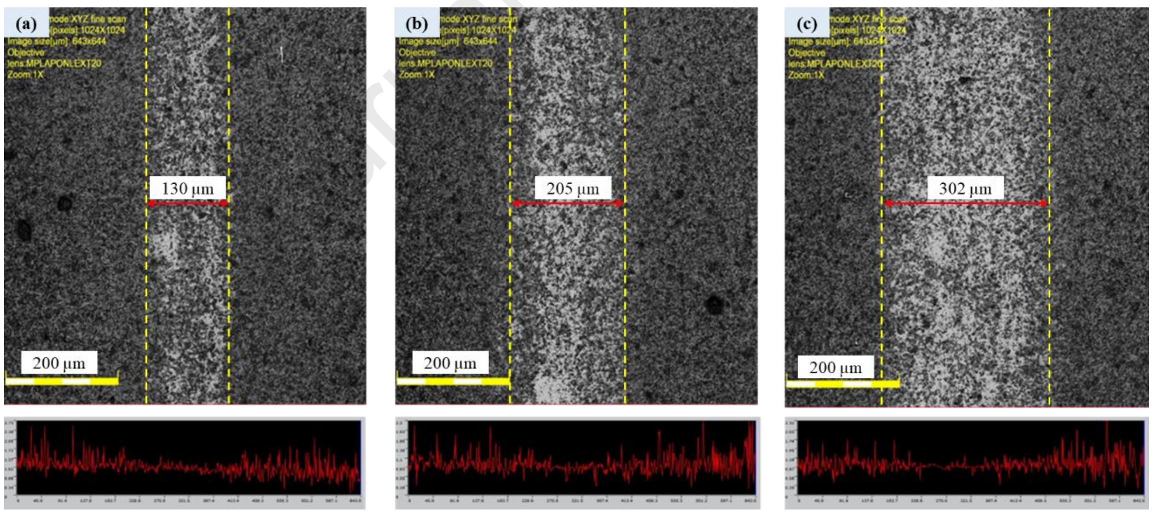

Fig. 12. Wear tracks and surface profiles on the nanodiamond composite film-coated silicon carbide substrate at varying sliding durations

Table 1 Comparison between NDC coatings and other coatings for mechanical seals applications.

Materials	Counter-body	Surface coating	Load (N)	Sliding Speed (m/s)	Temp. (°C)	RH (%)	CoF	Specific wear rate ($mm^3/N·m$)
SiC disk [73]	Si_3N_4 ball	Without coating	3	0.056	Ambient	-	0.04	-
		With one-layer diamond coating					0.14	-
		With multilayer diamond coating					0.07	-
SiC disk	Si_3N_4 ball	Without coating [42]	2	0.05	Ambient	20-25	0.24	$7.5*10^{-5}$
		With GLC coating (Ti interlayer) [41]				-	0.06	$6.5*10^{-7}$
		With GLC coating (Si interlayer) [42]				20-25	0.07	$5.2*10^{-7}$
(C/C) composites substrate	SiC ball	SiC coating [80]	2	0.1	25	50-60	0.43-0.48	$4.68*10^{-5}$
					600	-	0.65-0.75	Without obvious wear
					800	-	0.5-0.6	$1.51*10^{-3}$
SiC disk [81]	Si_3N_4 ball	Without coating	5	0.02	Ambient	40-50	0.4 ± 0.12	10^{-5}
		With CDC coating					0.08	Too low to measure
SiC disk [82]	Steel ball (SAE52100)	With CDC coating without dechlorination	5	0.02	20-21	49-51	0.3	-
		With CDC coating with dechlorination					0.15	-
SiC substrate (Current study)	SiC ball	Without coating	2.94	0.2	Ambient	49-51	1.22	-
		With NDC coatings					0.15 ± 0.03	Without obvious wear

4. Conclusion

In addressing the imperative requirement for enhancing the longevity and efficiency of mechanical seals in alignment with sustainability criteria, this study focuses on depositing a robust nanodiamond composite (NDC) film on SiC substrates utilizing the CAPD method. The NDC films, deposited at a rate of 2.6 μm/hr with a thickness of 1.1 μm, exhibited a remarkably smooth (Ra=60 nm) and uniform surface, influenced by the initial substrate roughness. Raman spectroscopy confirmed the presence of a nanodiamond phase with abundant grain boundaries and the formation of SiC intermetallic compounds. These grain boundaries acted as obstacles for microcrack initiation, enhancing film toughness, as demonstrated by the absence of delamination even under a load of 150 kg in the Rockwell test.

Nanoindentation tests unveiled outstanding hardness (48.5 GPa) and Young's modulus (496.7 GPa) alongside minimal plastic deformation (H/E=0.098), underlining the applicability of NDC films in settings that required durability and wear resistance. In tribological assessments conducted in ambient environments without lubrication, a progressive evolution in wear behaviour transpired, culminating in the establishment of a steady and low CoF at 0.18 for a 20 min test. This sustained and low CoF was ascribed to the diminished surface roughness of NDC, and the creation of a tribo-layer facilitated by abundant grain boundaries and the rehybridization of carbon sp^3 to sp^2 bonding, markedly amplifying sliding property and wear resistance.

Despite the SiC counter-body exhibiting escalating deteriorated wear resistance with increasing sliding periods, the NDC films showcased a smoothed track surface with negligible wear, even at the longest sliding period of 60 minutes over 720 m. The NDC asperities caused grooves, facilitating stress concentration and resulting in deteriorating wear resistance of the SiC counter-body while enhancing the film wear resistance.

The systematic exploration of mechanical properties and tribological performance of NDC film underscores their potential in advancing sustainable mechanical seals. This research contributes valuable insights into the realm of wear-resistant and adherent NDC films, promising prolonged machinery longevity, enhanced operational efficiency and lower engineering waste for mechanical seals. These results lay the foundation for further advancements in the development and application of NDC coatings in diverse industrial settings.

CRediT authorship contribution statement

Mohamed Egiza: Project administration, Conceptualization, Formal analysis, Writing-Original draft preparation, **Mohamed R. Diab**: Validation, Visualization, Methodology, **Abdul Wasy Zia**: Writing- Reviewing and Editing, **Koki Murasawa**: Methodology, **Nadimul Faisal:** Supervision, Writing- Reviewing and Editing, **Tsuyoshi Yoshitake**: Supervision, Funding acquisition.

Declaration of competing interest

The authors declare that they have no known competing financial interests or personal relationships that could have appeared to influence the work reported in this paper.

Data availability

Data will be made available on request.

Acknowledgement

This study received partial financial support from JSPS KAKENHI Grant Nos. JP19H02436 and 21K18830. Additional funding was provided by the Osawa Scientific Studies Grants Foundation, Advanced Machining Technology & Development Association, JST A-STEP Stage II (seed development type AS2915051S)

References

[1] S.S. Camargo, J.R. Gomes, J.M. Carrapichano, R.F. Silva, C.A. Achete, Silicon-incorporated diamond-like coatings for Si3N4 mechanical seals, Thin Solid Films, 482 (2005) 221-225.

[2] M.W. Brown, R.H.J. Warring, Seals and sealing handbook, (1995).

[3] A.V. Sumant, A.R. Krauss, D.M. Gruen, O. Auciello, A. Erdemir, M. Williams, A.F. Artiles, W. Adams, Ultrananocrystalline Diamond Film as a Wear-Resistant and Protective Coating for Mechanical Seal Applications, Tribology Transactions, 48 (2005) 24-31.

[4] K. Nadolny, W. Kapłonek, M. Sutowska, P. Sutowski, P. Myśliński, A. Gilewicz, B. Warcholiński, Moving towards sustainable manufacturing by extending the tool life of the pine wood planing process using the AlCrBN coating, Sustainable Materials and Technologies, 28 (2021) e00259.

[5] G.M. Krolczyk, R.W. Maruda, J.B. Krolczyk, S. Wojciechowski, M. Mia, P. Nieslony, G. Budzik, Ecological trends in machining as a key factor in sustainable production – A review, Journal of Cleaner Production, 218 (2019) 601-615.

[6] W. Zhang, S. Yamashita, H. Kita, Progress in tribological research of SiC ceramics in unlubricated sliding-A review, Materials & Design, 190 (2020) 108528.

[7] A.J. Ruys, Silicon Carbide Ceramics: Structure, Properties and Manufacturing, Elsevier, 2023.

[8] X. Liu, P. Lu, H. Wang, Y. Ren, X. Tan, S. Sun, H. Jia, Morphology and structure of Ti-doped diamond films prepared by microwave plasma chemical vapor deposition, Applied Surface Science, 442 (2018) 529-536.

[9] S. Jahanmir, D.E. Deckman, L.K. Ives, A. Feldman, E. Farabaugh, Tribological characteristics of synthesized diamond films on silicon carbide, Wear, 133 (1989) 73-81.

[10] A. Erdemir, G.R. Fenske, Tribological Performance of Diamond and Diamondlike Carbon Films at Elevated Temperatures, Tribology Transactions, 39 (1996) 787-794.

[11] K. Miyoshi, R.L.C. Wu, A. Garscadden, Friction and wear of diamond and diamondlike carbon coatings, Surface and Coatings Technology, 54-55 (1992) 428-434.

[12] A.M. Kovalchenko, J.W. Elam, A. Erdemir, J.A. Carlisle, O. Auciello, J.A. Libera, M.J. Pellin, D.M. Gruen, J.N. Hryn, Development of ultrananocrystalline diamond (UNCD) coatings for multipurpose mechanical pump seals, Wear, 270 (2011) 325-331.

[13] F. Mubarok, J.M. Carrapichano, F.A. Almeida, A.J.S. Fernandes, R.F. Silva, Enhanced sealing performance with CVD nanocrystalline diamond films in self-mated mechanical seals, Diamond and Related Materials, 17 (2008) 1132-1136.

[14] G.A. Jones, On the tribological behaviour of mechanical seal face materials in dry line contact: Part II. Bulk ceramics, diamond and diamond-like carbon films, Wear, 256 (2004) 433-455.

[15] Y. Du, F. Xie, J. Wang, B. Xu, H. Chen, B. Yan, Y. Wu, W. Huang, H. Li, Dry Friction Properties of Diamond-Coated Silicon Carbide, Materials (Basel), 16 (2023).

[16] C.S. Abreu, M. Amaral, A.J.S. Fernandes, F.J. Oliveira, R.F. Silva, J.R. Gomes, Friction and wear performance of HFCVD nanocrystalline diamond coated silicon nitride ceramics, Diamond and Related Materials, 15 (2006) 739-744.

[17] M. Vila, J.M. Carrapichano, J.R. Gomes, S.S. Camargo, C.A. Achete, R.F. Silva, Ultra-high performance of DLC-coated Si3N4 rings for mechanical seals, Wear, 265 (2008) 940-944.

[18] S.-J. Cho, K.-R. Lee, K. Yong Eun, J. Hee Hahn, D.-H. Ko, Determination of elastic modulus and Poisson's ratio of diamond-like carbon films, Thin Solid Films, 341 (1999) 207-210.

[19] R.K.Y. Fu, Y.F. Mei, M.Y. Fu, X.Y. Liu, P.K. Chu, Thermal stability of metal-doped diamond-like carbon fabricated by dual plasma deposition, Diamond and Related Materials, 14 (2005) 1489-1493.

[20] Y. Wang, L. Wang, G. Zhang, S.C. Wang, R.J.K. Wood, Q. Xue, Effect of bias voltage on microstructure and properties of Ti-doped graphite-like carbon films synthesized by magnetron sputtering, Surface and Coatings Technology, 205 (2010) 793-800.

[21] A.M. Ali, T. Deckert-Gaudig, M. Egiza, V. Deckert, T. Yoshitake, Near- and far-field Raman spectroscopic studies of nanodiamond composite films deposited by coaxial arc plasma, Applied Physics Letters, 116 (2020) 041601.

[22] K. Hanada, T. Yoshida, Y. Nakagawa, T. Yoshitake, Formation of ultrananocrystalline diamond/amorphous carbon composite films in vacuum using coaxial arc plasma gun, Japanese journal of applied physics, 49 (2010) 125503.

[23] T. Yoshitake, A. Nagano, S. Ohmagari, M. Itakura, N. Kuwano, R. Ohtani, H. Setoyama, E. Kobayashi, K. Nagayama, Near-edge x-ray absorption fine-structure, x-ray photoemission, and

Fourier transform infrared spectroscopies of ultrananocrystalline diamond/hydrogenated amorphous carbon composite films, Japanese journal of applied physics, 48 (2009) 020222.

[24] J. He, J.M. Schoenung, Nanostructured coatings, Materials Science and Engineering: A, 336 (2002) 274-319.

[25] M.R. Diab, M. Egiza, K. Murasawa, S. Ohmagari, H. Naragino, T. Yoshitake, Revealing mechanical and structural properties of Si-doped nanodiamond composite films through applied biasing voltages on WC − Co substrates, International Journal of Refractory Metals and Hard Materials, 119 (2024) 106518.

[26] M. Egiza, K. Murasawa, A.M. Ali, Y. Fukui, H. Gonda, M. Sakurai, T. Yoshitake, Enhanced hardness of nanocarbon films deposited on cemented tungsten carbide substrates by coaxial arc plasma deposition owing to employing silicon-doped graphite targets, Japanese Journal of Applied Physics, 58 (2019) 075507.

[27] M. Egiza, A.M. Ali, M.R. Diab, N. Hemaya, K. Murasawa, T. Yoshitake, Synthesis and comprehensive synchrotron-based structural analysis of Si-doped nanodiamond composite films deposited on cemented carbide, Surface and Coatings Technology, (2023).

[28] M. Egiza, H. Naragino, A. Tominaga, K. Murasawa, H. Gonda, M. Sakurai, T. Yoshitake, B-doped nanodiamond composite hard coatings deposited on cemented carbide: Mechanical, structural, and tribological properties, International Journal of Refractory Metals and Hard Materials, 114 (2023).

[29] A.M. Ali, M. Egiza, K. Murasawa, Y. Fukui, H. Gonda, M. Sakurai, T. Yoshitake, Negative bias effects on deposition and mechanical properties of ultrananocrystalline diamond/amorphous carbon composite films deposited on cemented carbide substrates by coaxial arc plasma, Diamond and Related Materials, 96 (2019) 67-73.

[30] N. Khanna, J. Wadhwa, A. Pitroda, P. Shah, J. Schoop, M. Sarıkaya, Life cycle assessment of environmentally friendly initiatives for sustainable machining: A short review of current knowledge and a case study, Sustainable Materials and Technologies, 32 (2022) e00413.

[31] I.S. Jawahir, J. Schoop, Y. Kaynak, A.K. Balaji, R. Ghosh, T. Lu, Progress Toward Modeling and Optimization of Sustainable Machining Processes, Journal of Manufacturing Science and Engineering, 142 (2020).

[32] D. Griggs, M. Stafford-Smith, O. Gaffney, J. Rockström, M.C. Öhman, P. Shyamsundar, W. Steffen, G. Glaser, N. Kanie, I. Noble, Sustainable development goals for people and planet, Nature, 495 (2013) 305-307.

[33] M. Egiza, M. Ragab Diab, A.M. Ali, K. Murasawa, T. Yoshitake, Sustainable super-hard and thick nanodiamond composite film deposited on cemented carbide substrates with an interfacial Al-interlayer, Materials Letters, 364 (2024).

[34] L. Osman, A. Zkria, A.M. Ali, S. Nagano, H. Naragino, T. Yoshitake, Synergistic effects of optimal negative bias-enhanced growth of quenched-produced diamond films on titanium substrates, Applied Physics Express, 16 (2023) 075501.

[35] M. Egiza, A.M. Ali, M.R. Diab, N. Hemaya, K. Murasawa, T. Yoshitake, Synthesis and comprehensive synchrotron-based structural analysis of Si-doped nanodiamond composite films deposited on cemented carbide, Surface and Coatings Technology, 471 (2023) 129867.

[36] A.M. Ali, M. Egiza, K. Murasawa, H. Sugita, T. Deckert-Gaudig, V. Deckert, T. Yoshitake, Effects of substrate temperature and intermediate layer on adhesion, structural and mechanical

properties of coaxial arc plasma deposition grown nanodiamond composite films on Si substrates, Surface and Coatings Technology, 417 (2021) 127185.

[37] N.H. Faisal, R. Ahmed, Y.Q. Fu, Y.O. Elakwah, M. Alhoshan, Influence of indenter shape on DLC film failure during multiple load cycle nanoindentation, Materials Science and Technology, 28 (2024) 1186-1197.

[38] L. Wang, Y. Liu, H. Chen, M. Wang, Nanoindentation-induced deformation behaviors of tetrahedral amorphous carbon film deposited by cathodic vacuum arc with different substrate bias voltages, Applied Surface Science, 576 (2022).

[39] W. Dai, Y. Shi, Q. Wang, J. Wang, Smooth diamond-like carbon films prepared by cathodic vacuum arc deposition with large glancing angles, Diamond and Related Materials, 141 (2024) 110672.

[40] J. Qi, C.Y. Chan, I. Bello, C.S. Lee, S.T. Lee, J.B. Luo, S.Z. Wen, Film thickness effects on mechanical and tribological properties of nitrogenated diamond-like carbon films, Surface and Coatings Technology, 145 (2001) 38-43.

[41] Y. Wang, L. Wang, Q. Xue, Improvement in the tribological performances of Si3N4, SiC and WC by graphite-like carbon films under dry and water-lubricated sliding conditions, Surface and Coatings Technology, 205 (2011) 2770-2777.

[42] Y. Wang, L. Wang, Q. Xue, Improving the tribological performances of graphite-like carbon films on Si3N4 and SiC by using Si interlayers, Applied Surface Science, 257 (2011) 10246-10253.

[43] W. Zhang, S. Yamashita, H. Kita, Progress in tribological research of SiC ceramics in unlubricated sliding-A review, Materials & Design, 190 (2020).

[44] P. Hollman, H. Björkman, A. Alahelisten, S. Hogmark, Diamond coatings applied to mechanical face seals, Surface and Coatings Technology, 105 (1998) 169-174.

[45] P.J. Kelly, R.D. Arnell, M.D. Hudson, A.E.J. Wilson, G. Jones, Enhanced mechanical seal performance through CVD diamond films, Vacuum, 61 (2001) 61-74.

[46] A. Erdemir, G.R. Fenske, A.R. Krauss, D.M. Gruen, T. McCauley, R.T. Csencsits, Tribological properties of nanocrystalline diamond films, Surface and Coatings Technology, 120-121 (1999) 565-572.

[47] A. Gupta, D. Paramanik, S. Varma, C. Jacob, CVD growth and characterization of 3C-SiC thin films, Bulletin of Materials Science, 27 (2004) 445-451.

[48] P.J.S.C.M. Colomban, Processing, A.i.E. Devices, M. Mukherjee, Ed, SiC, from amorphous to nanosized materials, the exemple of SiC fibres issued of polymer precursors, (2011) 161-186.

[49] D.-J. Won, M.O. Ramirez, H. Kang, V. Gopalan, N.F. Baril, J. Calkins, J.V. Badding, P.J.A. Sazio, All-optical modulation of laser light in amorphous silicon-filled microstructured optical fibers, Applied Physics Letters, 91 (2007).

[50] P.P. Dey, A. Khare, Tailoring of stoichiometry and band-tail emission in PLD a-SiC thin films by varying He deposition pressure, SN Applied Sciences, 2 (2020) 1059.

[51] C.-H. Cheng, C.-L. Wu, Y.-H. Lin, W.-L. Yan, M.-H. Shih, J.-H. Chang, C.-I. Wu, C.-K. Lee, G.-R. Lin, Strong optical nonlinearity of the nonstoichiometric silicon carbide, Journal of Materials Chemistry C, 3 (2015) 10164-10176.

[52] A.M. Ali, M. Egiza, K. Murasawa, H. Sugita, T. Deckert-Gaudig, V. Deckert, T. Yoshitake, Effects of substrate temperature and intermediate layer on adhesion, structural and mechanical properties of coaxial arc plasma deposition grown nanodiamond composite films on Si substrates, Surface and Coatings Technology, 417 (2021) 11.

[53] J. Birrell, J.E. Gerbi, O. Auciello, J.M. Gibson, J. Johnson, J.A. Carlisle, Interpretation of the Raman spectra of ultrananocrystalline diamond, Diamond and Related Materials, 14 (2005) 86-92.

[54] A.C. Ferrari, J. Robertson, Origin of the 1150−cm−1 Raman mode in nanocrystalline diamond, PHYSICAL REVIEW B, 63 (2001) 121405(R).

[55] A.C. Ferrari, J. Robertson, Raman spectroscopy of amorphous, nanostructured, diamond–like carbon, and nanodiamond, Philosophical Transactions of the Royal Society of London. Series A: Mathematical, Physical and Engineering Sciences, 362 (2004) 2477-2512.

[56] K. Aoki, K. Suzuki, K. Ishii, K. Takanashi, T. Komukai, K. Oura, T. Hirao, Formation of Nanoscale Diamond Particles without Substrate Heating by Cathodic Arc Deposition, Japanese Journal of Applied Physics, 44 (2005) L746.

[57] Q. Lin, S. Chen, Z. Ji, Z. Huang, Z. Zhang, B. Shen, Deposition of mirror-like surface finish ultrananocrystalline diamond films on tungsten carbide by optimizing the substrate pretreatment, Surface and Coatings Technology, 394 (2020) 125885.

[58] A. Dychalska, P. Popielarski, W. Franków, K. Fabisiak, K. Paprocki, M. Szybowicz, Study of CVD diamond layers with amorphous carbon admixture by Raman scattering spectroscopy, Mater. Sci.-Pol, 33 (2015) 799-805.

[59] R.J. Nemanich, S.A. Solin, First- and second-order Raman scattering from finite-size crystals of graphite, Physical Review B, 20 (1979) 392-401.

[60] I.I. Vlasov, V.G. Ralchenko, E. Goovaerts, A.V. Saveliev, M.V. Kanzyuba, Bulk and surface-enhanced Raman spectroscopy of nitrogen-doped ultrananocrystalline diamond films, phys. stat. sol. (a), 203 (2006) 3028-3035.

[61] I. Harada, Y. Furukawa, M. Tasumi, H. Shirakawa, S. Ikeda, Spectroscopic studies on doped polyacetylene and β-carotene, The Journal of Chemical Physics, 73 (2008) 4746-4757.

[62] X. Li, X. Wu, P. Wu, J. Yuan, Y. Zhu, Effects of polishing media on the surface chemical and micromechanical properties of SiC, Computational Materials Science, 233 (2024) 112753.

[63] L. Xue, G. Feng, G. Wu, F. Dong, K. Liang, R. Li, S. Wang, S. Liu, Study of deformation mechanism of structural anisotropy in 4H–SiC film by nanoindentation, Materials Science in Semiconductor Processing, 146 (2022) 106671.

[64] Q. Jun, L. Jianbin, W. Shizhu, W. Jing, L. Wenzhi, Mechanical and tribological properties of non-hydrogenated DLC films synthesized by IBAD, Surface and Coatings Technology, 128-129 (2000) 324-328.

[65] S. Chowdhury, E. de Barra, M.T. Laugier, Study of mechanical properties of CVD diamond on SiC substrates, Diamond and Related Materials, 13 (2004) 1625-1631.

[66] S. Chowdhury, E. de Barra, M.T. Laugier, Hardness measurement of CVD diamond coatings on SiC substrates, Surface and Coatings Technology, 193 (2005) 200-205.

[67] S.J. Bull, E.G. Berasetegui, An overview of the potential of quantitative coating adhesion measurement by scratch testing, Tribology International, 39 (2006) 99-114.

[68] D.-d. Ma, Y.-p. Xue, J. Gao, Y. Ma, S.-w. Yu, Y.-s. Wang, C. Xue, H.-j. Hei, B. Tang, Effect of Ta diffusion layer on the adhesion properties of diamond coating on WC-Co substrate, Applied Surface Science, 527 (2020) 146727.

[69] R. Dumpala, N. Kumar, C.R. Kumaran, S. Dash, B. Ramamoorthy, M.S. Ramachandra Rao, Adhesion characteristics of nano- and micro-crystalline diamond coatings: Raman stress mapping of the scratch tracks, Diamond and Related Materials, 44 (2014) 71-77.

[70] H. Cicek, A. Keles, Y. Totik, I. Efeoglu, Adhesion and multipass scratch characterization of Ti:Ta-DLC composite coatings, Diamond and Related Materials, 83 (2018) 80-86.

[71] S. Du, K. Zhang, M. Wen, P. Ren, Q. Meng, C. Hu, W. Zheng, Tribochemistry dependent tribological behavior of superhard TaC/SiC multilayer films, Surface and Coatings Technology, 337 (2018) 492-500.

[72] J. Musil, Hard and superhard nanocomposite coatings, Surface and Coatings Technology, 125 (2000) 322-330.

[73] N. Chen, L. Pu, F. Sun, P. He, Q. Zhu, J. Ren, Tribological behavior of HFCVD multilayer diamond film on silicon carbide, Surface and Coatings Technology, 272 (2015) 66-71.

[74] R. Rani, K.J. Sankaran, K. Panda, N. Kumar, K. Ganesan, S. Chakravarty, I.N. Lin, Tribofilm formation in ultrananocrystalline diamond film, Diamond and Related Materials, 78 (2017) 12-23.

[75] T.W. Scharf, I.L. Singer, Quantification of the Thickness of Carbon Transfer Films Using Raman Tribometry, Tribology Letters, 14 (2003) 137-145.

[76] S. Zhang, Y. Fu, H. Du, X.T. Zeng, Y.C. Liu, Magnetron sputtering of nanocomposite (Ti,Cr)CN/DLC coatings, Surface and Coatings Technology, 162 (2003) 42-48.

[77] G.G. Adams, M. Nosonovsky, Contact modeling — forces, Tribology International, 33 (2000) 431-442.

[78] W. Zheng, J. Sun, C. Ma, Q. Yu, The Theoretical Basis of Face Contact Pressure Design of the Zero-Leakage Mechanical Seal, Coatings 12 (2022) 536.

[79] L.J. Martini, Practical seal design, Routledge, 2018.

[80] C. Zishan, L. Hejun, F. Qiangang, Q. Xinfa, Tribological behaviors of SiC/h-BN composite coating at elevated temperatures, Tribology International, 56 (2012) 58-65.

[81] J. Sui, J. Lu, Formulated self-lubricating carbon coatings on carbide ceramics, Wear, 271 (2011) 1974-1979.

[82] F. Gao, J. Lu, W. Liu, Tribological Behavior of Carbide-derived Carbon Coating on SiC Polycrystal against SAE52100 Steel in Moderately Humid Air, Tribology Letters, 27 (2007) 339-345.

Highlights

- CAPD deposited eco-friendly smooth NDC coating at 2.6 μm/hr rate.
- NDC displayed hardness of 48.5 GPa and Young's modulus of 496.7 GPa.
- Raman verified NDC's nanostructure and SiC intermetallic bonding.
- EDS confirmed SiC intermetallic compound formation at the interface.
- NDC exhibits superior adhesion in scratch (Lcr > 60 N) and Rockwell tests.
- NDC maintains low COF (0.18) with minimal wear on SiC counter-body.